

# Shock Induced Damage onto Free-Standing Objects in an Earthquake

Haider AlAbadi, Joe Petrolito, Nelson Lam, and Emad Gad

**Abstract**—In areas of low to moderate seismicity many building contents and equipment are not positively fixed to the floor or tied to adjacent walls. Under seismic induced horizontal vibration, such contents and equipment can suffer from damage by either overturning or impact associated with rocking. This paper focuses on the estimation of shock on typical contents and equipment due to rocking. A simplified analytical model is outlined that can be used to estimate the maximum acceleration on a rocking object given its basic geometric and mechanical properties. The developed model was validated against experimental results. The experimental results revealed that the maximum shock acceleration can be underestimated if the static stiffness of the materials at the interface between the rocking object and floor is used rather than the dynamic stiffness. Excellent agreement between the model and experimental results was found when the dynamic stiffness for the interface material was used, which was found to be generally much higher than corresponding static stiffness under different investigated boundary conditions of the cushion. The proposed model can be a beneficial tool in performing a rapid assessment of shock sensitive components considered for possible seismic rectification.

**Keywords**—Impact, shock, earthquakes, rocking, building contents, overturning.

## I. INTRODUCTION

**I**N regions of high seismicity, the intention is to ensure that all building contents and installations are secured in position, and preferably fully restrained from movement in the event of an earthquake. The required strength of the restraint is normally specified as the product of the component mass and the peak acceleration developed in the component according to the basic principles of mechanics (e.g. [1]–[3]). On the other hand, in regions of low to moderate seismicity where building contents are typically *free-standing*, the provisions in contemporary codes of practice for the design of structures have not given realistic models for evaluating the seismic performance behavior of such objects. This is because of limitations with the commonly used quasi-static and dynamic

modal analysis methods for modeling the motion behavior of an object that rotates (or “rocks”) within the limits of overturning. Numerous investigations have been undertaken by different research groups over many years to analyze the rocking and/or sliding motions of free-standing objects [4]–[16]. Simplified simulation algorithms have accordingly been developed to model the displacement time-history of rocking motion [17], [18]. Simplified hand calculation methods based on linearization have also been proposed to relate the maximum displacement limit of rocking to certain base motion parameters [16] and [19], [20]. Thus, much of the attention in the various cited articles has been devoted to motions and the risk of overturning.

Past investigations and developed methods cannot model the damage, if any, that is sustained during rocking. Impact-tolerance, or the ability to safely withstand rocking (or overturning), drops and bangs in projected earthquake scenarios, is becoming an increasingly important aspect of the reliability of contemporary built facilities [21], [22]. The safety and well-being of the community can also be compromised by damage of this nature, and more so if the equipment carries a post-disaster recovery function.

This paper is concerned with estimating the impact acceleration that is generated by the impact of a rocking object on the floor, or on an adjacent obstacle, when excited into rocking motion in an earthquake. Sliding is assumed not to occur, implying that the base horizontal acceleration has not surpassed the coefficient of friction between the base of the object and the flooring surface. A steel cabinet for housing electronic/computer equipment was the subject of the investigation. Accurate prediction of the shock level is important in terms of modeling damage to the cabinet and its contents. Two types of impact have been considered in the investigation, namely (i) impact generated by the overturning of an object, or the rocking of a squat object (Figs. 1 (a) and (b)) and (ii) impact generated by rocking motion of a slender object as its base repetitively pounds on the floor (Fig. 1 (c)). The illustrated case study features the use of rubber pads that were attached to the underside of the cabinet to cushion the impact. This modeling technique would allow for further investigations on other available flooring products (e.g. carpets, vinyl, etc.). Given that the floor supporting the cabinet was without any floor coverings, the rubber pads were by far the most deformable parts, and hence they absorbed most of the energy generated by the pounding. The cabinet itself was assumed to be rigid, so that any energy loss associated with its deformation can be neglected. Importantly, results from physical full-scale experiments on the cabinet have been used

H. Al Abadi is with the Department of Civil engineering and Physical Sciences, La Trobe University, Bendigo, Victoria 3552, Australia (corresponding author phone: 61-3-5444-7608; fax: 61-5444-7878; e-mail: h.alabadi@latrobe.edu.au).

J. Petrolito is with the Department of Civil engineering and Physical Sciences, La Trobe University, Bendigo, Victoria 3552, Australia (e-mail: j.petrolito@latrobe.edu.au).

N. Lam is with the Department of Infrastructure, The University of Melbourne, Parkville, Victoria 3010, Australia (e-mail: ntkl@unimelb.edu.au).

E. Gad is with the Faculty of Engineering and Industrial Sciences, Swinburne University of Technology, Hawthorn, Victoria 3122, Australia (e-mail: egad@swin.edu.au).

to verify the proposed analytical model (Section III). Results of a parametric investigation into the static and dynamic stiffness properties of the rubber cushion are also presented to guide the selection of input parameters (Section IV). The proposed methodology can be readily adapted to cases where there are floor coverings, and it can be further developed for modeling damage in other types of containers as well as gravity structures.

The impact model proposed is applied in Section V for generating Shock Spectra Curves (SRS) for building contents experiencing rocking motion due to seismic-induced horizontal vibration. These curves can be directly used for estimating the level of acceleration developed at the edge of the impact between an object and the floor by simply defining the object's dimensions (i.e. height and width).

## II. MODEL FOR DETERMINING IMPACT ACCELERATION

This paper is concerned with estimating the impact acceleration generated by the impact of a free-standing object on the floor, or adjacent obstacle, when excited into rocking motion in an earthquake.

The objective of the modeling approach to be introduced in this section is to estimate the impact acceleration  $a_{edge}$  generated in a free standing object experiencing one of the impact scenarios shown in Figs. 1 (a)-(c). By considering the objects as being "rigid" so that any energy loss associated with its deformation can be neglected, and that the nearby media in contact is much more flexible than the objects themselves, the key unknown to solve is the dynamic stiffness  $k$  of any cushion material that is in place between the objects and the floor, or an adjacent obstacle. The material properties of the cushion material used for floor coverings (e.g., carpet or vinyl), are not well documented as they are nontypical engineering materials. Accordingly, experiments would need to be conducted for estimating the potential impact acceleration generated by impact on these materials. For any type of cushioning material, a simplified experiment represented by dropping a rigid lumped mass ( $m$ ) from a height  $\Delta h_{cg}$  as shown in Fig. 1 (d) can be used.

The value of maximum impact force ( $F$ ) generated by the three scenarios shown in Fig. 1 is a function of the amount of energy absorbed by the cushion. This amount of energy absorption can be equated to the amount of loss in potential energy at the instant of impact. The maximum acceleration force ( $F$ ) experienced on impact by the vertically dropped object as well as the impact scenarios shown in Figs. 1 (a) and (b) (where the overturning motion of the object is halted by the impact) are relatively straightforward to analyse in contrast to the impact scenario shown Fig. 1 (c), where the overturning motion of the object continues after impact. Provided that the mass ( $m$ ) and dropped height ( $\Delta h_{cg}$ ) of the vertically dropped lumped mass is equal to that of the overturned objects, the equation of moment equilibrium taken about the pivotal edge of the object at the instance of impact is

$$F \cdot d = m \cdot a \cdot d = I_o \ddot{\theta} \quad (1)$$

where  $d$  is the distance between the pivotal edge and the point of impact,

$$I_o = \frac{3}{4} \cdot m \cdot R^2 \quad (2)$$

$$\ddot{\theta} = a_{edge}/d \quad (3)$$

$F$  would have been the reaction force had the rotation been halted by the impact as for the impact scenarios shown in Figs. 1 (a) and (b). The value of the impact force under the rocking motion scenario (Fig. 1 (c)) is different as a smaller force  $F_s$  is developed so that the rotation continues).

Assuming linear elastic behavior of the cushion stiffness ( $k$ ), it can be shown that:

$$\frac{F_s^2/2k}{F^2/2k} = \frac{F_s^2}{F^2} = 1 - R_D^2 \implies F = F_s/\sqrt{1 - R_D^2} \quad (4)$$

where  $1 - R_D^2$  is the proportion of kinetic energy retained in the cabinet following the impact and  $R_D (= \dot{\theta}_2/\dot{\theta}_1)$  is the ratio of the angular velocity prior to and immediately following the impact.

Substituting (2)-(4) into (1) and rearranging the terms, gives

$$a_{edge} = \frac{3}{4} \frac{1}{\sqrt{1 - R_D^2}} \left(\frac{d}{R}\right)^2 a \quad (5)$$

Equation (6) below, which estimates the value of  $R_D$  as a function of  $d/R$ , has been derived by [23]. It was originally derived as a function of the coefficient of restitution [9]. The expression, which is based on equating the angular momentum of the rotating object prior to and immediately following the changeover of the pivotal point at the instance of impact, is

$$R_D = \frac{\dot{\theta}_2}{\dot{\theta}_1} = 1 - \frac{3}{8} \left(\frac{d}{R}\right)^2 \quad (6)$$

Using equation (6), the impact acceleration ( $a_{edge}$ ) generated at the edge of an overturned cabinet can be inferred from results taken from an experiment that simply involves dropping a lumped mass  $m$  onto the cushion material.

With situations of low-moderate intensity impact, where the stiffness properties of the cushion material can be taken as linear-elastic, the value of  $a$  that is required for input into (5) can be estimated by equating the amount of energy absorbed in the form of strain energy and the loss of potential energy of the object at the point of impact [23]. This gives

$$a = \sqrt{\frac{2 \cdot k \cdot g \cdot \Delta h_{cg}}{m}} \quad (7)$$

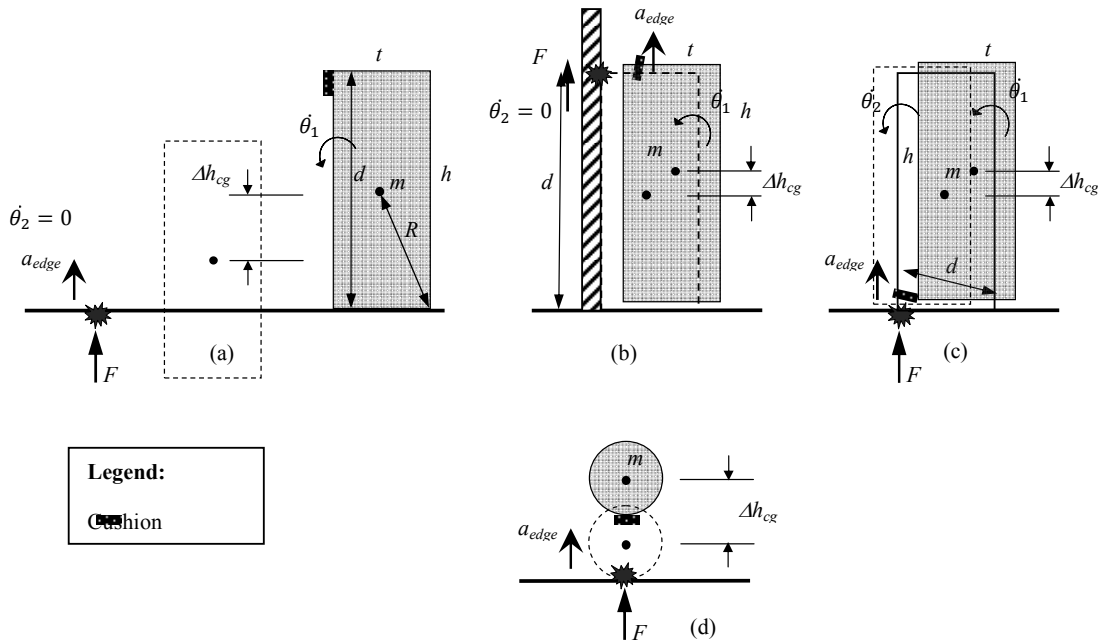


Fig. 1 Types of impact scenarios

In summary, for any of the impact scenarios considered in this paper (Fig. 1), the impact acceleration ( $a_{edge}$ ) generated at the edge of the cabinet can be inferred from the value of  $a$  measured from the experimental results of a vertically dropped lumped mass using (5) and (7). When the rotation motion is halted by the impact (i.e.  $\dot{\theta}_2 = 0 \Rightarrow R_D = 0$ ), as for the cases of impact scenarios Figs. 1 (a) and (c), (5) can be simplified to

$$a_{edge} = \frac{3}{4} \left(\frac{d}{R}\right)^2 a \quad (8)$$

### III. EXPERIMENTAL VERIFICATIONS

Full-scale physical impact tests have been carried out on a cabinet. The cabinet used was of dimensions 2.3m (height)  $\times$  0.9m (width) and 0.6m (depth). The cabinet was made up of a rigid steel frame covered by metal sheets. The cabinet, which was displaced in the direction of the “depth”, was fitted (glued) with four rubber pads each of which was placed on the underside of its four corners as shown in Fig. 2. Given that these rubber pads were more deformable than the cabinet and the floor, most of the energy was absorbed by the pads. Five experiments were conducted, where the cabinet was raised to a pre-determined value of vertical displacement ( $\Delta h_{cg}$ ) as listed in Table I. Two accelerometers were mounted on the cabinet and directly above the corners where impact was made with the floor and cushioned by the rubber. Measurements were taken as the cabinet was dropped for rocking. An example time trace of the measured acceleration is shown in Fig. 3. The peak values taken from the two accelerometers were recorded

and averaged. The averaged results are listed in the far right hand column of Table I. Calculations were performed to predict the value of the emulated acceleration  $a$  using (7) for each of the given value of  $\Delta h_{cg}$  and for  $m = 140\text{kg}$ . The dynamic spring constant of the attached pads was taken as 4380N/mm (i.e. 2190N/mm per pad) based on results from dynamic testing to be described in Section IV. The impact acceleration value  $a_{edge}$  was calculated for each case using (5).

TABLE I  
COMPARISON OF PREDICTED AND MEASURED ACCELERATION VALUES

Test no.	$\Delta h_{cg}$ (mm)	$a$ (g) from (7)	$a_{edge}$ (g) from (5)	$a_{edge}$ (g) from direct measurements
1	16	10.1	4.6	4
2	16	10.1	4.6	4.1
3	27	13.1	5.9	6
4	27	13.1	5.9	6.3
5	32	14.3	6.5	7

### IV. EXPERIMENTAL INVESTIGATION OF STIFFNESS PROPERTIES OF RUBBER CUSHION

In the experimental study presented in Section III, the dynamic stiffness value of the square rubber pad (cushion) was taken to be 2190N/m per piece, which measured 78mm  $\times$  78mm  $\times$  20mm thick. This stiffness value was based on results derived from an experimental investigation involving both static and dynamic testing. Details of the investigation are described in this section.

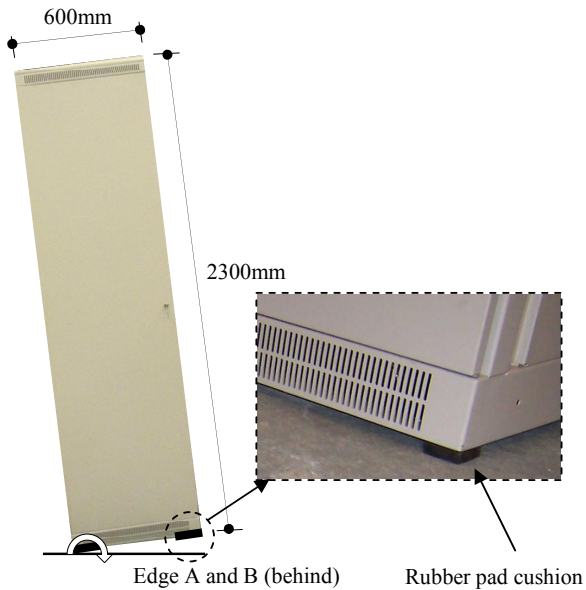


Fig. 2 Test setup for the physical full-scale experiments

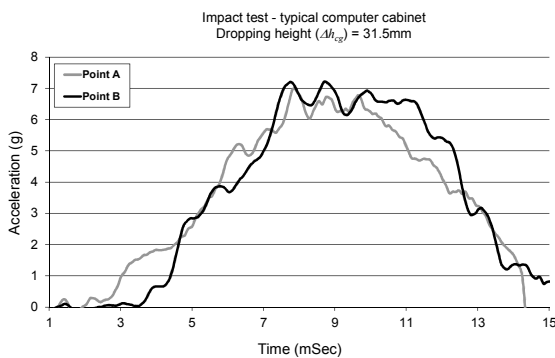


Fig. 3 An example of measured acceleration at impact

In the static experiments, the square rubber pad was laid flat on a hard surface and then subjected to a monotonic increase in uniform pressure applied from above. The statically applied force measured by the load cell was correlated with the displacement measured on LVDT transducers.

In the dynamic experiments, the rubber pad was pounded from above by a 12mm thick steel plate that weighed 365 grams. The amount of shock impact acceleration experienced by the steel plate was logged by accelerometers attached to its upper surface. The displacement time-history of the compression of the rubber was obtained by double-integration of the accurately recorded (and baseline corrected) acceleration values. The acceleration-displacement and dynamic force-displacement relationships were obtained using this technique.

Rubber pad specimens were tested repetitively with both static and dynamic loads based on the following boundary conditions that controlled the degree of restraints on the rubber: (i) the rubber pad was secured to the flat surface by

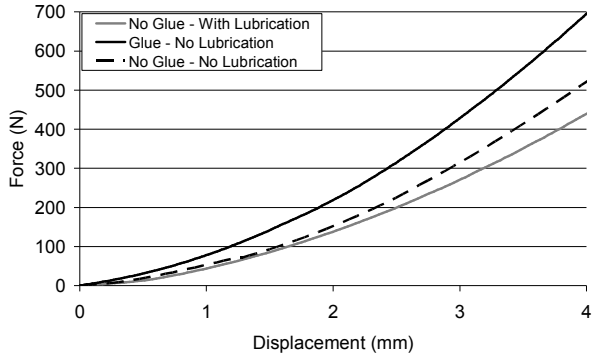
glue (consistent with conditions on the cabinet), (ii) the rubber pad was simply placed on the flat surface without the use of glue and (iii) lubricants were applied onto the surface of the rubber pad, which was then placed on the flat surface without the use of glue. The objective was to eliminate frictional restraining forces on the rubber.

The initial set of static and dynamic tests was conducted with a square rigid steel plate as an impactor. In the second set of tests, the steel plate was replaced by a rigid metal sphere of 19mm radius weighing 365 grams.

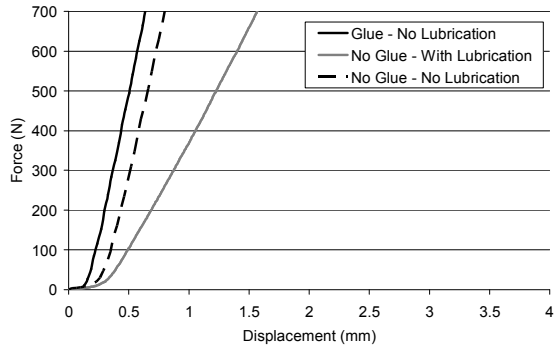
The force-displacement relationships obtained from the static tests are shown for comparison in Fig. 4 (a) and (b). The static stiffness properties of the rubber cushion was shown to be sensitive to the boundary conditions of the rubber pad and the nature of the impactor. It is shown by the comparative plots that the restraining actions generated by the glue and the frictional forces developed between the rubber and impactor both contributed to a notable increase in the static stiffness values.

The dynamic force-displacement relationships obtained from the two sets of impact experiments are presented in Figs. 5 and 6, respectively. The observed dynamic stiffness values of the rubber cushion for given boundary conditions and impactor type were generally much higher than the corresponding static stiffness values. Previous studies related to polymeric structural foams under compressive impact loading showed that dynamic stiffness becomes higher as the rate of deformation increases [24]-[27]. Dynamic stiffness values of twice the static stiffness values were recorded with some tests. Thus, the dynamic stiffness properties of the rubber could also be affected by the restraining actions of both the glue and friction as observed with the static experiments. However, the ratio of the dynamic/static stiffness could not be generalized given that the value of this ratio is highly variable across the different scenarios. Linear-elastic behaviour of the rubber cushion may be assumed for the flat plate impact scenarios. A dynamic spring constant of 2190 N/m has been identified for conditions that were consistent with that of the metal cabinet (Fig. 6 (a)).

Trends observed from tests employing the flat plate as impactor were similar to those employing the rigid metal sphere as impactor but non-linear (Hertzian) behavior was far more pronounced with the second set of test results (Fig. 6 (a)-(c)).

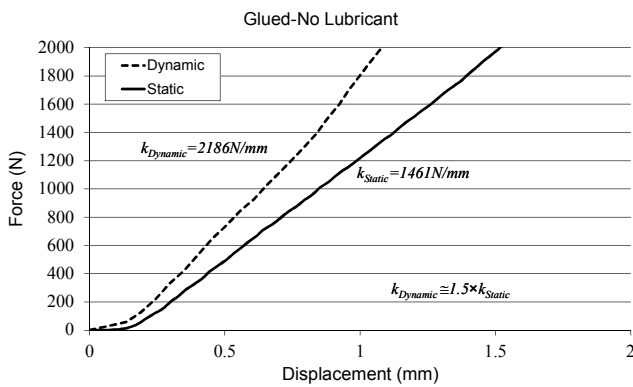


(a) spherical geometry surface.

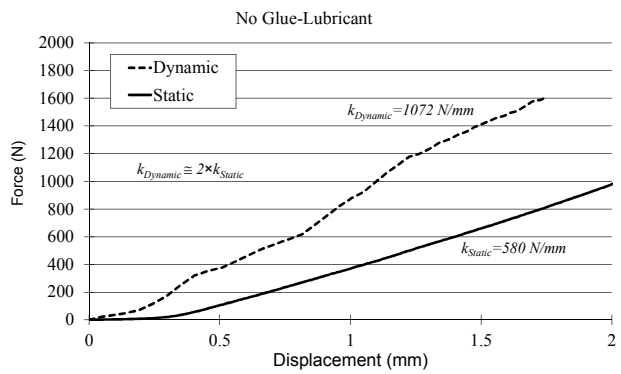


(b) flat geometry surface

Fig. 4 Results of static tests

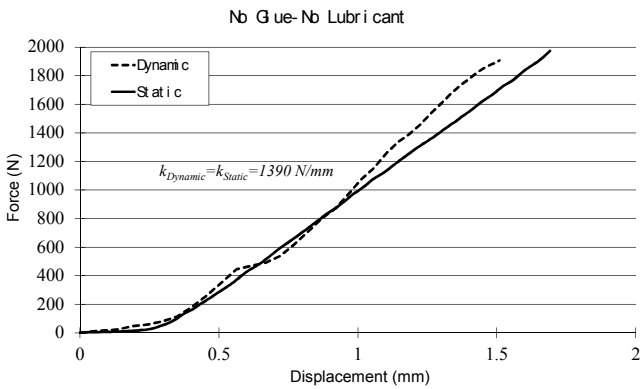


(a) Glued and no lubricant applied

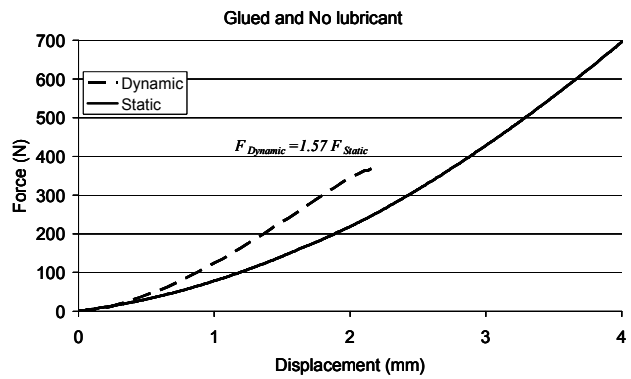


(c) No glued used but lubricant was applied

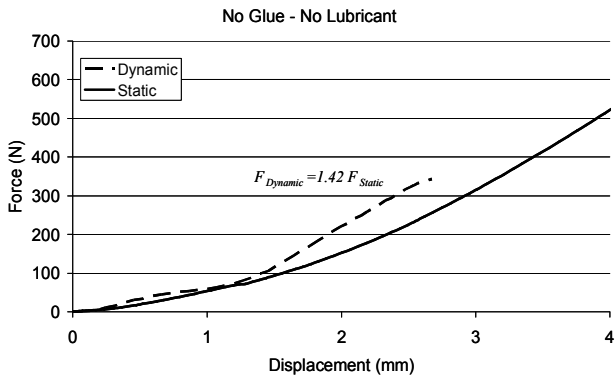
Fig. 5 Results of dynamic tests (flat plate impactor)



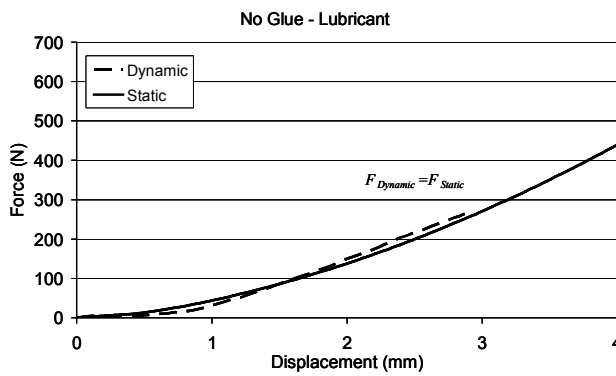
(b) No glued nor lubricant applied



(a) Glued and no lubricant applied



(b) No glued nor lubricant applied



(c) No glued used but lubricant was applied

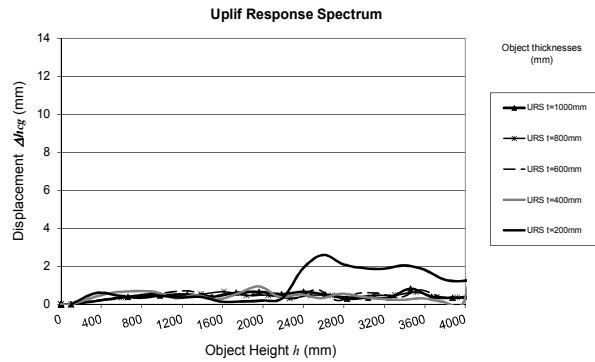
Fig. 6 Results of dynamic tests (spherical impactor)

V. SHOCK RESPONSE SPECTRA CURVES FOR FREE STANDING OBJECTS

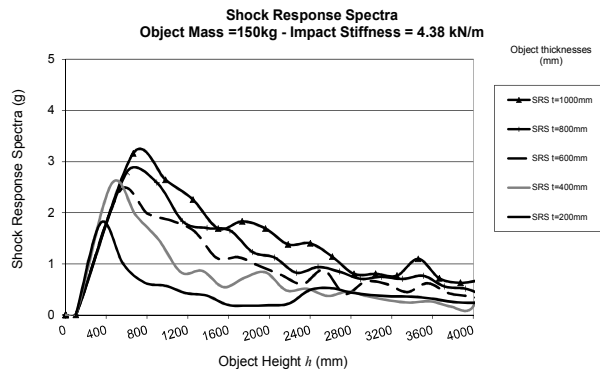
The impact model proposed and verified in this paper is applied in this section for generating Shock Response Spectra (SRS) curves for building contents experiencing rocking motion due to floor seismic-induced horizontal vibration. These curves can be simply used for estimating the level of shock  $a_{edge}$  developed at the edge of impact between an object and the floor by defining the object's dimensions (i.e. height and width).

SRS curves have been developed from the Uplift Response Spectra (URS) curves of building contents. The URS represents the maximum uplift displacement experienced by objects subjected to floor excitations as shown in Fig. 6. The URS curves were generated by using the non-linear time history analysis rocking model [12], and they are a function of the object's height, thickness and the floor excitation. By applying the impact model procedure for calculating the level of shock developed in the rocking object (Section II), URS curves can be converted to SRS curves. Fig. 7 shows examples of SRS curves for objects considered to be mounted at mid-height and roof levels of a generic 30-storey building. A synthetic accelerogram simulating a 500 year return period earthquake in Melbourne, Australia, for a class D site was

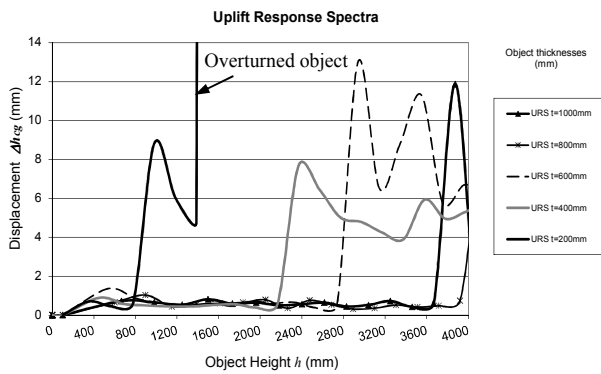
used as the input motion at ground level. In addition to the object's geometry and the base applied excitations, the stiffness of the flooring material at the vicinity of impact between the object and floor (including the stiffness of the object's supporting legs) and the mass of the object are required to be defined for obtaining such curves. In this case study, the mass of the object was taken as 150kg and the stiffness of the flooring material at the pivotal edge was taken as 4380N/m, which is a typical value for a rubber pad material. From Fig. 7, the maximum acceleration level ( $a_{edge}$ ) induced into the free standing objects, installed at the mid-height of the building, can be estimated at about 3.5g, while objects located at the roof level could reach a maximum acceleration level of 5g. These values can be compared with the tolerance levels of various components to examine the potential for malfunctioning. SRS curves also indicate the risks of overturning for the rocking objects, as was predicted to be the case for a 200mm thick object, with height more than 1500mm and located at the roof level of the modeled building.



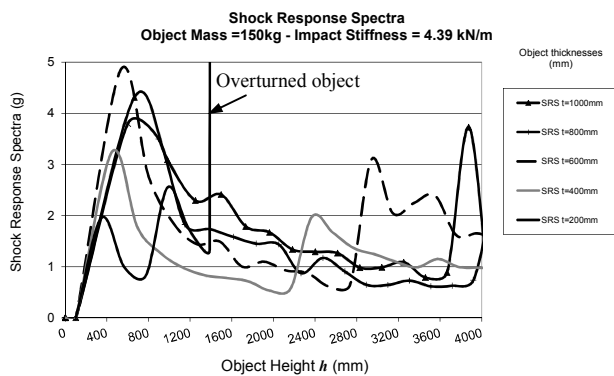
(a) URS at mid-height level of a generic 30-storey building



(b) SRS at roof level of a generic 30-storey building



(c) URS at roof level of a generic 30-storey building



(d) SRS at roof level of a generic 30-storey building

Fig. 7 URS and SRS for floor mounted building contents

## VI. CONCLUSION

Relationships have been derived for predicting the amount of impact acceleration ( $a_{edge}$ ) that is generated by the impact of a steel cabinet on the floor, or on a neighboring obstacle, when excited into rocking motion in an earthquake. Equation (5) in conjunction with (7) enables the value of  $a_{edge}$  to be predicted for any given geometrical ratio  $t/R$  of the cabinet and the value of  $a$ , which is the impact acceleration emulated by simply dropping a lumped mass onto the cushion material. For low-moderate intensity impact in which linear-elastic behavior may be assumed, the value of  $a$  can be determined once the values of the spring constant  $k$  (characterizing the dynamic stiffness of the rubber cushion) and the initial potential energy of the lifted cabinet are known. The results of a parametric investigation provided insight into the sensitivity of the value of the static and dynamic stiffness to changes in boundary conditions and the type of impactor used. The dynamic stiffness values were generally much higher than the static stiffness values for the same boundary conditions, but the ratio of dynamic/static stiffness could not be generalized. As an application for the proposed model, Shock Response Spectra (SRS) curves are presented, which can be simply used to assess the level of shock induced damage onto free-standing objects in an earthquake.

## REFERENCES

- [1] FEMA 356, Prestandard and Commentary for Seismic Rehabilitation of Buildings. Prepared by the American Society of Civil Engineers for the Federal Emergency Management Agency. FEMA, 2000.
- [2] IBC, *International Code Council. International building Code, U.S.A.*, 2000.
- [3] AS/NZS 1170.4, *Australian Standard for Structural Design Actions, Part 4: Earthquake Actions in Australia*. 2005.
- [4] G.W.Housner, "The Behaviour of inverted pendulum structures," *Bulletin of the Seismological Society of America*, 53 (2), 403-417. 1963.
- [5] S.C.S.Yim, A.K.Chopra, and J.Penzien, "Rocking Response of Rigid Blocks to Earthquakes," *Earthquake Engineering and Structural Dynamics* 122(7), 69093. 1980.
- [6] M.Aslam, W.G.Godden, and D.T.Scalise, "Earthquake rocking response of rigid bodies," *Journal of the Structural Division*, 106, 377-392, 1980.
- [7] Y.Ishiyama, "Motions of rigid bodies and criteria for overturning by earthquake excitations," *Earthquake Engineering and Structural Dynamics*, 10, pp. 635-650. 1982.
- [8] S.J.Hogan, "On the dynamics of rigid-block motion under harmonic motion," *Proc. R. Soc. Lond.*, 425, 441-476. 1989.
- [9] P. R. Lipscombe, *Dynamics of rigid block structures*. Ph.D. thesis, University of Cambridge, 1990.
- [10] N. Makris and Y.Roussos, "Rocking Response and Overturning of Equipment Under Horizontal Pulse-Type Motions," *Pacific Earthquake Engineering Research Center PEER 1998*, Report No. 5, 1998.
- [11] N.Makris and D.Konstantinidis, "The Rocking Spectrum and the Shortcomings of Design Guidelines," *Pacific Earthquake Engineering Research Center PEER 2001*, Report No. 7, 2001.
- [12] H.Al Abadi, *Unrestrained Building Contents in Regions of Low-Moderate Seismicity*. Ph.D. thesis, Civil Engineering Dept., The University of Melbourne, Melbourne, 2008.
- [13] H. Al Abadi, N.Lam, and E.Gad, "A simple displacement-based model for predicting seismically induced overturning," *Journal of Earthquake Engineering*, 2006 10(6), 775-814, 2006.
- [14] H.Al Abadi, N.T.K.Lam, E.F.Gad, and A.M.Chandler, "Earthquake Floor Spectra for Unrestrained Building Components," *International Journal of Structural Stability and Dynamics*, 4 (3), 361-377, 2004.
- [15] D.Franke, N.Lam, E.Gad, and A.Chandler, "Seismically Induced Overturning of Objects and Filtering Effects of Buildings," *International Journal of Seismology and Earthquake Engineering*, 7 (2), 95-108, 2005.
- [16] B.Kafle, N.Lam, E.Gad, and J.Wilson, "Displacement controlled rocking behaviour of rigid objects," *Earthquake Engineering and Structural Dynamics*, 40, 1653-1669, 2011.
- [17] N.Lam, M.Griffith, J. Wilson, and K. Doherty, "Time History Analysis of URM walls in out-of-plane flexure," *Journal of Engineering Structures*, 25 (6), 743-754, 2003.
- [18] M.C.Griffith, N.T.K. Lam, J.L. Wilson, and K.Doherty, "Experimental Investigation of Unreinforced Brick Masonry Walls in Flexure," *Journal of Structural Engineering*, 130(3), 423-432, 2004.
- [19] K.Doherty, M.Griffith, N.T.K. Lam, and J.L.Wilson, "Displacement-Based Analysis for out-of plan bending of seismically loaded unreinforced masonry walls," *Earthquake Engineering and Structural Dynamics*, 31(4), 833-850, 2002.
- [20] E.Lumantarna, N.T.K. Lam, J.L.Wilson, and M.C.Griffith, "Inelastic Displacement Demand of Strength Degraded Structures," *Journal of Earthquake Engineering*, 14: 487-511, 2010.
- [21] N.T.K.Lam and E.G.Gad, "Overturning of Non-structural Components in Low-moderate Seismicity Regions. Special Issue on Earthquake Engineering in Low-Moderate Seismicity Regions of Southeast Asia and Australia," *Electronic Journal of Structural Engineering*, 121-132. 2008.
- [22] S.Goyal, E. K. Buratynski, and G. W. Elko, "Role of Shock Response Spectrum in Electronic Product Suspension Design," *The International Journal of Microcircuits and Electronic Packaging*, vol. 23, no. 2, pp. 182-190, Second Quarter 2000.
- [23] H.Al Abadi, N.Lam, E.Gad, and J. Petrolito, "A Simple Model for Estimating Shocks in Unrestrained Building Contents in an Earthquake," *Journal of Earthquake Engineering*, in press.
- [24] M.Avalle, G. Belingardi, and R. Montanini, "Characterization of polymeric structural foams under compressive impact loading by means of energy-absorption diagram," *International Journal of Impact Engineering*, 25, 455-472, 2001.

- [25] R.R.A.Cousins, "Theory of the Impact Behaviour of Rate-Dependent Padding Materials," *Journal of Applied Polymer Science*, 20, 2893-2903, 1976.
- [26] O.Ramon and J.Miltz, "Prediction of Dynamic Properties of Plastic Foams from Constant-Strain Rate Measurements," *Journal of Applied Polymer Science*, 40, 1683-1692, 1990.
- [27] R.W.Shuttleworth, V.O.Shestopal, and P.C.Goss, "Open-Cell Flexible Polyurethane Foams: Comparison of Static and Dynamic Compression Properties," *Journal of Applied Polymer Science*, 30, 333-343, 1985.